946 *Macromolecules* **2009**, *42*, 946−956

Use of a Poly(ethylene oxide) MacroRAFT Agent as Both a Stabilizer and a Control Agent in Styrene Polymerization in Aqueous Dispersed System

A. Martins dos Santos,*,‡ T. Le Bris,† C. Graillat,† F. D'Agosto,*,† and M. Lansalot*,†

Université de Lyon, Univ. Lyon 1, CPE Lyon, CNRS UMR 5265, Laboratoire de Chimie, Catalyse, Polymères et Procédés (C2P2), LCPP team, 43 Bd du 11 Novembre 1918, F-69616, Villeurbanne, France, and Laboratório de Polímeros, Departamento de Engenharia Química, Escola de Engenharia de Lorena—USP, Estrada Municipal do Campinho, s/n°, CP 116, 12.602.810, Lorena (SP), Brasil

Received September 17, 2008; Revised Manuscript Received December 12, 2008

ABSTRACT: A poly(ethylene oxide)-based macromolecular agent for reversible addition-fragmentation chain transfer (PEO-RAFT, 2 000 $g \cdot mol^{-1}$) was synthesized and used as a stabilizer and a control agent in the miniemulsion polymerization of styrene. Using 2,2′-azobis(isobutyronitrile) as initiator, stable polystyrene (PS) particles sterically stabilized by the PEO segments were obtained with almost complete conversion after 22 h. Molar masses increased linearly with conversion although rather broad molar mass distributions were obtained due to the presence of several populations of PEO-*b*-PS block copolymers. However, dynamic light scattering analyses showed a significant increase in particle diameter with conversion and the ratio of the number of particles to the number of droplets (N_p/N_d) was thus lower than one indicating that the system did not follow a true miniemulsion process. Transmission electron microscopy additionally revealed the presence of holes inside the formed particles suggesting that block copolymer PEO-*b*-PS could be buried inside the particles during the polymerization. Varying the concentration and the nature of the initiator did not lead to an improvement of the molar mass distribution, while a decrease in polymerization temperature to 40 °C enabled to keep the particle size constant throughout the polymerization with values close to the starting droplet diameter as expected for a true miniemulsion.

Introduction

The successful synthesis of latex particles relies on a judicious choice of the main reagents involved in their elaboration. Among them, the surfactant plays a key role in the formation and growth of the particles by ensuring their colloidal stability. Three types of surfactant are usually described: (a) electrostatic stabilizers, which are charged low molar mass molecules able to provide electrostatic repulsion between the particles, (b) steric stabilizers, which are polymer chains with both hydrophilic and hydrophobic domains, and able to induce entropic repulsion between polymeric chains of two different particles, and (c) electrosteric stabilizers, which combine the characteristics of the two first classes.

Due to their size, steric and electrosteric stabilizers (or macromolecular stabilizers) show many advantages over low molar mass ones, such as improved stability under freezing conditions or under high shear, or preventing from diffusion issues during film-formation. Indeed, macromolecular stabilizers strongly adsorbed onto the surface of the particles[1−4] or even anchored via a covalent bond[5] are less inclined to desorb or migrate compared to conventional low molar mass surfactants like sodium dodecyl sulfate (SDS). To be covalently linked to the particles, the surfactant must carry a group able to participate to one of the key-steps of the free radical polymerization process (initiation, propagation, termination or transfer reactions) that leads to the formation of the chains incorporated into the particles. According to the reaction in which they are involved, these reactive surfactants are referred to as *inisurf* (initiation),[6] *surfmer* (propagation)[3] or *transurf* (transfer).[7,8] In these particular cases, the surfactant not only plays a key role in the formation of the particles and the functionalization of their surface, but also becomes actor in the synthesis of the polymer chains which will form the particles.

If the two first classes of reactive surfactants have been deeply studied, only a few works deal with the synthesis and the use of transurfs,[2] and for most of them a thiol transferring group is involved. For instance, Fifield et al.[9] synthesized sodium 10-mercapto-1-decanesulfonate, a low molar mass transurf which was used in emulsion polymerization of styrene to produce stable colloids containing sulfonate ionic surface functional groups. Thiol-ended poly(ethylene oxide) (PEO) or poly(vinyl acetate-*co*-vinyl alcohol) chains were also successfully used as macromolecular transurf in styrene dispersion[10−12] or emulsion[7] polymerization. In fact, the high transferring nature of the thiol function[13] leads to a high reactivity of the transurf in the dispersing phase. As a result, although the *in situ* formation of amphiphilic block copolymers—able to act as the proper surfactant and to stabilize the formed particles—is taking place, the hydrophobic segment is not long enough to provide the block copolymers with sufficient surface activity, leading to a poor anchorage of the surfactant at the surface of the particles. To overcome this drawback, and favor a more gradual incorporation of the transurf, less transferring groups such as ones operating via an addition-fragmentation mechanism, namely derivatives of dimer of methyl methacrylate[8,14] or allyl sulfides,[1] have been introduced at the end of low molar mass surfactant or macromolecular chains and used in emulsion polymerization of styrene.

Instead of using less transferring end groups, the use of reversible chain transfer agents consists in an interesting alternative to efficiently anchor the transurf onto the particle. This strategy has very recently emerged and benefits from the unprecedented advances in controlled radical polymerization techniques.[15−18] These techniques include the reversible addi-

---

* Corresonding authors. E-mail: (A.M.d.S.) amsantos@dequi.eel.usp.br; (F.D.) dagosto@lcpp.cpe.fr; (M.L.) lansalot@lcpp.cpe.fr.

‡ Laboratório de Polímeros, Departamento de Engenharia Química, Escola de Engenharia de Lorena—USP.

† Université de Lyon, Univ. Lyon 1, CPE Lyon, CNRS UMR5265, Laboratoire de Chimie, Catalyse, Polymères et Procédés (C2P2), LCPP team.

10.1021/ma802117h CCC: $40.75

Scheme 1. Chemical Structure of the Poly(ethylene oxide)-Based Macromolecular Agent for Reversible Addition−Fragmentation Chain Transfer (PEO-RAFT)

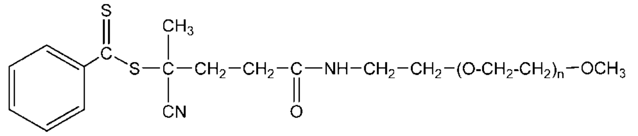

tion-fragmentation chain transfer (RAFT) process[19] which relies on the use of thiocarbonyl thio compounds of structure Z−C(=S)−SR, which are very efficient reversible chain transfer agents acting as control agents (RAFT agents). The proper choice of R and Z groups depends on the monomer to polymerize and not only influences the kinetics of the polymerization, but also enables an accurate functionalization of the α- and ω-chain ends of the polymer chains (via R and Z, respectively). Notably, RAFT recently allowed the synthesis of various amphiphilic copolymers subsequently used as efficient surfactant in emulsion[20,21] or miniemulsion[22−24] polymerization.

As mentioned above, an original and challenging approach consists of taking advantage of the reactivity of the thiocarbonyl thio end group of hydrophilic (co)polymers (i.e., hydrophilic macroRAFT agents) for controlling the formation of the particles. Indeed, like the above-mentioned thiol-ended chains used in emulsion polymerization,[7] hydrosoluble macroRAFT agents (either directly obtained by RAFT polymerization or via chemical modification of preformed polymers) can act as a transurf during an emulsion polymerization by forming an amphiphilic block copolymer *in situ* which is capable to stabilize the nascent particles. The very first example of this type relies on the use of poly(acrylic acid) as a macroRAFT agent in the synthesis of poly(butyl acrylate) core poly(acrylic acid) shell particles[25,26] under butyl acrylate feed conditions. Using a similar procedure, Božović-Vukić et al.[27] obtained stable particles starting from a RAFT synthesized poly(4-vinylpyridine) used in the emulsion copolymerization of styrene and acrylonitrile in a semicontinuous process. Simplified procedures were further proposed for batch emulsion polymerization of various monomers by using presynthesized hydrophilic macroRAFT agents such as polysoap,[28] the protonated form of poly(diethylaminoethyl methacrylate) (PDEAEMA),[29] a double hydrophilic block copolymer of poly(ethylene oxide)-*b*-poly(dimethylaminoethyl methacrylate) (PEO-*b*-PDMAEMA),[30] dextran,[31] polyacrylamide[32] and PEO.[33] Stable latex particles of polystyrene (PS),[28−30,33] poly(butyl acrylate)[26,33] or poly(vinyl acetate)[31] were obtained in each case and sometimes[33] additional control over the molar mass of the chains constituting the particles was achieved, thus demonstrating the versatility and the potential of this novel approach which does not require the use of additional free surfactant.

Previous work in our group indicated that this approach could be extrapolated to dispersion polymerization.[34] We would like to report here on the first attempt to our knowledge to apply it in miniemulsion polymerization of styrene. This paper focuses on the synthesis of polystyrene particles via miniemulsion polymerization using a PEO macroRAFT agent (Scheme 1) as both stabilizer of the particles and control agent of the free radical process.

Experimental Section

Materials. Water was deionized before use (Purelab Classic UV, Elga LabWater). Styrene (S, 99%, Aldrich) was distilled under vacuum. Hexadecane (HD, 99%, Acros Organics), potassium persulfate (KPS, 99+%, Acros Organics), sodium metabisulfite (SMB, 97+%, Acros Organics), dilauroyl peroxide (LPO, 99%, Acros Organics) were used as received. 2,2′-Azobis(isobutyronitrile) (AIBN, Fluka, 98%) was recrystallized from ethanol at 40 °C. PEO-RAFT was synthesized by reacting the commercially available amino-PEO (PEO-NH_2, 2 000 $g \cdot mol^{-1}$, methoxy poly(ethylene glycol) amine, 99.99%, Fluka) according to the procedure described by dos Santos et al.[30]

Partitioning of PEO-RAFT between Water and Styrene. A mixture of styrene, water and PEO-RAFT of the same composition as in Latex 1 recipe (see Table 1) was vigorously stirred at 75 °C for 20 min and then left at the same temperature until complete separation of styrene and water. The amount of emulsifier in the aqueous phase was determined by gravimetric analysis, and the amount in styrene calculated by mass balance.

Miniemulsion Polymerization Procedure. Batch miniemulsion polymerizations of styrene were performed at 75 °C in a three-necked round-bottom flask equipped with a condenser and a nitrogen inlet. Styrene was first mixed with hexadecane and the initiator (if monomer-soluble, i.e., AIBN or LPO). This organic phase was then added to the aqueous phase (water and PEO-RAFT) under vigorous stirring. After 15 min, the resulting mixture was ultrasonicated (750W Vibracell 75042, amplitude 90%) for 2 min. The obtained stable miniemulsion was then transferred to the round-bottom flask and deoxygenated by purging with nitrogen for 30 min at room temperature. The introduction of the round-bottom flask into the preheated oil bath corresponded to time zero of the polymerization. A slightly different procedure was used with a water soluble initiator (i.e., KPS or KPS/SMB): the temperature was raised to 75 °C during the nitrogen purge, and the following addition of the initiator gave the zero time of the polymerization. The regular withdrawal of samples allowed us to follow the conversion of

Table 1. Summary of experimental conditions for miniemulsion polymerizations of styrene mediated by poly(ethylene oxide)-based macromolecular agent for reversible addition-fragmentation chain transfer (PEO-RAFT) at 75 °C[a]

expt	initiator[b]	[initiator] ($mol \cdot L^{-1}{}_{em}$)	[PEO-RAFT] ($mol \cdot L^{-1}{}_{em}$)	$conv_{t=7h}$ (%)	D_h[c](nm) − *Poly*	N_p ($mL^{-1}{}_{Latex}$)
Latex 1	AIBN	9.1×10^{-3}	2.2×10^{-3}	59[d]	358 − *0.08*	4.2×10^{12}
Latex 2	AIBN	9.2×10^{-3}	4.4×10^{-3}	42	224 − *0.13*	1.8×10^{13}
Latex 3	AIBN	9.1×10^{-3}	6.4×10^{-3}	33	178 − *0.24*	3.5×10^{13}
Latex 4	AIBN	4.6×10^{-3}	2.2×10^{-3}	40[e]	347 − *0.13*	4.7×10^{12}
Latex 5	AIBN	5.6×10^{-4}	2.2×10^{-3}	10[f]	633 − *0.44*	8.1×10^{11}
Latex 6	KPS	9.2×10^{-3}	2.2×10^{-3}	94	581 − *0.26*	9.4×10^{11}
Latex 7	KPS SMB	9.1×10^{-3} 9.4×10^{-3}	2.2×10^{-3}	87	325 − *0.05*	5.4×10^{12}
Latex 8	LPO	9.3×10^{-3}	2.2×10^{-3}	59	389 − *0.76*	3.3×10^{12}
Latex 9	KPS SMB	9.6×10^{-3} 9.6×10^{-3}	1.9×10^{-3}	43[g]	170 − *0.04*	3.5×10^{13}

[a] All experiments were carried out with 10 wt % of styrene; hexadecane = 5.2 wt %/styrene; $T = 75$ °C (except Latex 9, $T = 40$ °C). [b] k_d values (s^{-1}) are as follows. 2,2′-Azobis(isobutyronitrile) (AIBN): $k_d = 9.06 \times 10^{-5}$ s^{-1} (75 °C /styrene, from ref 43). Potassium persulfate (KPS): $k_d = 4.35 \times 10^{-5}$ s^{-1} (75 °C /water, from ref 44). KPS/Sodium metabisulfite (SMB): $k_d = 2.7 \times 10^{-4}$ s^{-1} (75 °C /water from ref 45). Dilauroyl peroxide (LPO): $k_d = 1 \times 10^{-4}$ s^{-1} (74.8 °C/styrene, from ref 43). [c] Obtained by dynamic light scattering. [d] 90% conversion achieved within 22 h ($D_h = 406$ nm; *Poly* = 0.12). [e] 86% conversion achieved within 22 h ($D_h = 403$ nm; *Poly* = 0.43). [f] 25% conversion achieved within 22.7 h ($D_h = 686$ nm; *Poly* = 0.23). [g] 94% conversion achieved within 23 h ($D_h = 174$ nm; *Poly* = 0.06).

monomer as a function of time and the evolution of molar masses and molar mass distributions as a function of monomer conversion.

Characterization Techniques. Monomer consumption was followed by gravimetric analysis of samples withdrawn from the polymerization medium at different times. The particle size (hydrodynamic diameter, D_h) and the dispersity of the sample (*Poly*- the higher this value, the broader the size distribution) were measured by dynamic light scattering (DLS, Zetasizer HS1000 from Malvern Instruments). The data were collected using the fully automatic mode of the Zetasizer system, and depending on the size distribution, either the monomodal analysis (the so-called cumulants analysis) or the Contin analysis was performed. The number of particles N_p ($mL^{-1}{}_{Latex}$) is calculated using D_h from DLS according to eq 1, with τ the solid content of the emulsion ($g \cdot mL^{-1}{}_{Latex}$) and ρ the density of the particles (taking into account the conversion).

$$N_p = \frac{6\tau}{\rho \pi D_h{}^3} \qquad (1)$$

The number of radicals per particle $\bar{n}$ is estimated using N_p and the concentration of propagating radicals $[P^\bullet]$ determined experimentally from the slope of $\ln[M]_0/[M]_t$ versus time curve (see equation (2), which gives the rate of polymerization R_p as function of $[P^\bullet]$, with k_p the rate constant of propagation ($L \cdot mol^{-1} \cdot s^{-1}$), $[M]_p$ the monomer concentration in the particles).

$$R_p = k_p[M]_p[P^\bullet] = k_p[M]_p \frac{\bar{n}N_p}{N_a} \qquad (2)$$

The latexes (diluted solution deposited on a Formvar-coated copper grid and allowed to evaporate) were further examined by transmission electron microscopy at an accelerating voltage of 80 kV (Philips CM 120, Centre Technologique des Microstructures (CTμ), Claude Bernard University, Villeurbanne, France). The number- and weight-average diameter ($\overline{D_n}$ and $\overline{D_w}$, respectively) as well as the particle size dispersity ($I_p = \overline{D_w}/\overline{D_n}$) were determined using AnalySIS software (Soft Imaging System).

Molar masses and molar mass distributions of the dried polymers were determined by size exclusion chromatography (SEC) using a modular system comprising a Waters 515 HPLC pump and an autosampler 717Plus (Waters). A precolumn (PLgel 5 μm) and three columns [two PLgel 5 μm Mixed C (300 × 7.5 mm^2) and one PLgel 5 μm 500 A (300 × 7.5 mm^2)] thermostatted at 30 °C were used with tetrahydrofuran (THF) as eluent at a flow rate of 1 $mL \cdot min^{-1}$. Waters 410 refractometer was used for detection and molar masses were calculated on the basis of a calibration curve using low polydispersity polystyrene standards.

The particles in their dry state were analyzed using differential scanning calorimetry (DSC). Appropriate amounts of samples were sealed in aluminum sample pans and were prepared by compression molding. DSC thermo-scans of the materials were then recorded under a dry nitrogen atmosphere at a heating rate of 10 °C min^{-1} from 20 to 130 °C, in two scans using a Setaram DSC 131 apparatus. The machine was first calibrated with a set of pure metals (mercury, indium, tin, lead, and zinc). Glass transition temperature (T_g) was obtained from the inflection point method, whereas the melting temperature (T_m) was taken at the endothermic maximum.

Results and Discussion

PEO-RAFT Mediated Miniemulsion Polymerization of Styrene. Prior to any polymerization experiment, the ability of PEO-RAFT to stabilize a miniemulsion of styrene in water was checked. Solutions of PEO-RAFT in water and hexadecane in styrene were mixed together at room temperature and sonicated. A miniemulsion exhibiting styrene droplet size close to 200 nm (determined by DLS measurements) and which was stable for at least 7 h (even if the particle size distribution became slowly broader; see Supporting Information) was obtained. The same procedure was also conducted with commercial hydroxylated PEO (PEO-OH). However, in this case, the sonication step did not allow the formation of a miniemulsion. These preliminary observations clearly show that enough PEO-RAFT molecules are located at the interface between styrene droplets and the aqueous phase to ensure the stabilization of the formed miniemulsion.

Following these preliminary stability studies, miniemulsion polymerization was then carried out with AIBN as initiator at 75 °C (Latex 1). The detailed experimental conditions and features of the final latex are provided in Table 1. 59% monomer conversion was reached within 7 h (and 90% conversion achieved after 22 h, Figure 1a) with a slight induction period of about 30 min. Samples were regularly withdrawn from the polymerization medium and analyzed by SEC. As shown by Figure 1b a shift of the corresponding SEC chromatograms toward higher molar masses with conversion is observed. Indeed, a linear evolution of M_n with conversion can be plotted up to high conversion while polydispersity indices (M_w/M_n) remain rather high (Figure 1c). The broad molar mass distribution (at least three populations can be identified at low conversion) suggests a quite complex polymerization mechanism. This also likely explains the discrepancies between theoretical M_n and experimental values observed in Figure 1c. Note that the best fit of experimental M_n is obtained by taking into account initiator derived chains with AIBN efficiency f set to 0.2 using the following equation:

$$M_{n,th} = m_{RAFT} + \frac{[M]_0 m_{styrene}}{[RAFT]_0 + 2f[I]_0(1 - e^{-k_d t})} x \qquad (3)$$

where $M_{n,th}$ is the theoretical number average molar mass, m_{RAFT} is the molar mass of the macroRAFT agent, $m_{styrene}$ is the molar mass of styrene, x is the fractional monomer conversion, $[M]_0$ is the initial monomer concentration, $[RAFT]_0$ is the initial macroRAFT agent concentration, $[I]_0$ is the initial initiator concentration, k_d is the decomposition rate coefficient of the initiator and t is the time. It should be noted that the concentrations in this expression are all with respect to the total organic phase.

Despite broad molar mass distribution, the corresponding chains seem to be living as attested by the chromatograms shift with conversion observed by SEC analyses (Figure 1b). If this is effectively the case, the final latex should only be composed of PEO-*b*-PS block copolymers. In order to investigate this last point, DSC measurements after two temperature treatments were performed on commercial PEO-OH (DSC1) and on a mixture of PEO-OH and PS homopolymer in the same weight ratio as in Latex 1 (DSC2), and compared to measurements carried out on Latex 1 (DSC3) (Figure 1d). As expected, DSC1 showed an endothermic effect corresponding to the melting of PEO (Tm = 59 °C). The same endothermic peak is observed for DSC2 with an additional glass transition temperature (Tg) around 110 °C corresponding to the Tg of PS homopolymer. The absence of melting of free PEO in DSC3 together with the low Tg observed (80 °C) compared to the Tg determined in DSC2 (110 °C) is a strong indication of the formation of block copolymers during the polymerization.

The particle diameter steadily increased during the polymerization, while the number of particles was divided by 10 (ratio of the number of particles to the number of initial droplets N_p/N_d close to 0.1) (Figure 1e). These observations rule out the possibility of particle formation via a true miniemulsion polymerization, and suggest, together with molar mass observations mentioned above as well as the quite broad particle size distribution observed by TEM (Figure 1f, $\overline{D_n}$= 373 nm, $\overline{D_w}/\overline{D_n}$= 1.07), that the complex polymerization mechanism that is taking place may be related to a partitioning of PEO-RAFT molecules between the organic and the aqueous phase. Indeed, in previous works, Rieger et al.[33] and our group[30] assessed the ability of a PEO-based dithioester macroRAFT agent to act as a precursor of stabilizer in an *ab initio* emulsion polymerization of styrene. In our case, the polymerization was very slow and less than 5% conversion was reached in 7 h. From the beginning of the polymerization, a pink organic layer was observed indicating that free PEO-RAFT was likely located in the monomer phase suggesting that PEO-RAFT was readily able to migrate between the different phases. Thus, to better comprehend our system we determined the partitioning of PEO-RAFT between water and styrene at 75 °C, and found that only 46 wt % of PEO-RAFT remained in the aqueous phase. As a result, although this value was determined in the absence of monomer droplets (no HD and no sonication step—see Experimental Section), PEO-RAFT may be located in various loci at the beginning of the polymerization: in the water, in the styrene droplets and at the water/droplets interface. Although hydrophobic, AIBN is able to initiate the polymerization in water (water solubility = 0.04 wt %[35]) and polymerization can thus take place in water, at the water/droplet interface and inside the droplets giving rise to several molar mass populations consistently with the obtained SEC data and the number and size of the obtained particles.

Whatever the mechanisms leading to their formation, sterically stabilized and uncharged particles composed of PS-*b*-PEO chains with controlled molar masses have been synthesized. The formation of these particles does not fully obey to a miniemulsion process, and drawing a clear picture of the mechanisms operating in this system would be so far quite risky, but it seems reasonable (i) to think that particles can be created as originally expected by the growth of PS segments from the interface of PEO-RAFT stabilized droplets (i.e., from PEO-RAFT), (ii) that PEO-*b*-PS formed in the aqueous phase could be efficiently captured by existing droplets/particles due to the large surface area available, (iii) that some of these droplets may act as reservoirs for already nucleated ones and/or more likely that coagulation of already formed particles may happen (this would explain the decrease of N_p), and (iv) not to exclude that side micellar nucleation could happen by self-assembly of PEO-*b*-PS copolymer forming in aqueous phase. The block copolymer formation requiring early chain transfer reactions would account for the observed induction period (see Figure 1a). As the polymerization seems however to remain under RAFT control, we further investigate the influence of different parameters on this system such as the PEO-RAFT concentration, the concentration and nature of the initiator and the polymerization temperature.

Influence of PEO-RAFT Concentration. The results in the previous section clearly showed the crucial role played by PEO segments in the stability of the final latex. In this section we will further focus on some aspects of the system. First, with the two-fold goal of increasing the rate of polymerization and narrowing the particle size distribution, experiments with higher initial concentration of PEO-RAFT (i.e., higher potential of particle stabilization) and a constant AIBN concentration were performed, and the results are shown in Figure 2 and Table 1 (Latex 2 and Latex 3).

Increasing PEO-RAFT concentration leads to a significant decrease of the polymerization rate (the slope of $\ln([M]_0/[M]_t)$ vs conversion decreases accordingly, data not shown) together with a slightly longer induction period (Figure 2a). This decrease in rate could be regarded as a possible RAFT retardation effect[36] that would be emphasized by the increasing amount of PEO-RAFT. Such a decrease in polymerization rate when increasing macroRAFT agent concentration was already reported in the literature. Indeed, Luo et al.[37] performed RAFT miniemulsion polymerization of styrene at 75 °C with hydrophobic PS-based macroRAFT agents (PS-RAFT), using potassium persulfate (KPS) as initiator, SDS as surfactant and hexadecane (HD) as hydrophobe. These experimental conditions were optimized to fit the assumptions of their kinetic model. The authors mentioned that increasing PS-RAFT concentration did not influence the number of particles, results which indicated that the observed retardation could not be adequately explained on this lone basis. The observed decrease of the (calculated) average number of radicals per particle $\bar{n}$ with PS-RAFT concentration was indeed put forward. Our results are different: although $\bar{n}$ decreases with PEO-RAFT concentration (Latex 1, $\bar{n} = 1$; Latex 2, $\bar{n} = 0.16$; Latex 3, $\bar{n} = 0.06$), the number of particles increases (Table 1). Note that similar observation has been reported in the case of a dextran-based macroRAFT agent used in ab initio emulsion polymerization of vinyl acetate.[31] Indeed, our system differs from the one studied by Luo et al.,[37] since we use a macroRAFT agent (with a hydrophilic PEO-based R group) which not only plays the role of the control agent but also of the surfactant. As a result, an increase in macroRAFT agent concentration will consistently lead to an increase in the number of particles, which has been experimentally observed. The decrease in polymerization rate can thus find its origin in the fact that the decrease of $\bar{n}$ seems to prevail on the increase of N_p and eventually on the kinetics (see eq 2). Considering the complexity of our system, it remains however difficult to further comment on the decrease of $\bar{n}$ and on any associated compartmentalization effect[17] and especially on whether and how compartmentalization of the propagating radicals may affect the polymerization rate and the controlled features of the system.

As expected in a controlled radical polymerization, the results in Figure 2b show that the higher the concentration of PEO-RAFT, the lower the molar masses. More surprisingly, TEM photos from Latex 2 revealed morphologies in which particles have lost their spherical shape and exhibited inside holes, distributions in size, shape and holes being quite inhomogeneous (Figure 2c). Direct TEM observation of Latex 3 was not possible due to the soft nature of the obtained particles. This kind of morphology has already been observed by several teams. Okubo et al.[38,39] reported a loss of the spherical shape of the particles together with an increasing number of domains with less contrast when increasing the concentration of the poly(oxyethylene) nonylphenyl ether emulsifier in styrene emulsion polymerization. Tauer et al. observed less contrast domains[40] in surfactant free styrene emulsion polymerization initiated with KPS in presence of a chain transfer agent[41] or employing symmetrical PEG azo inisurf in styrene emulsion polymerization.[42] Although a clear understanding of the formation of these "holes" is missing so far, the origin of these structures is likely associated with the presence and the incorporation of the PEO chains inside the PS particles either as homopolymers or as segments of a block copolymer. PEO and PS being incompatible, PEO may either go to the aqueous phase if it is a homopolymer or phase separate if it is part of a block copolymer which is our case. These hydrophilic chains would gather in a particular spot and water would accumulate there later leading to holes when the particles are analyzed under vacuum by TEM. This additional phenomenon complicates even more the interpretation of the mechanisms leading to the formation of the particles.

Influence of the Concentration and the Type of Initiator. In a next series of experiments, the effect of the variation of the initiator concentration was studied, using AIBN as initiator and a constant initial amount of PEO-RAFT (2.2×10^{-3} mol·$L^{-1}{}_{em}$). The results are shown in Figure 3. As expected, a decrease in AIBN concentration leads to a decrease of the polymerization rate, together with a longer induction period (Figure 3a). The radical flux being lowered, the nucleation of the particles is longer. This is best exemplified by Latex 5 for which the concentration of AIBN is too low

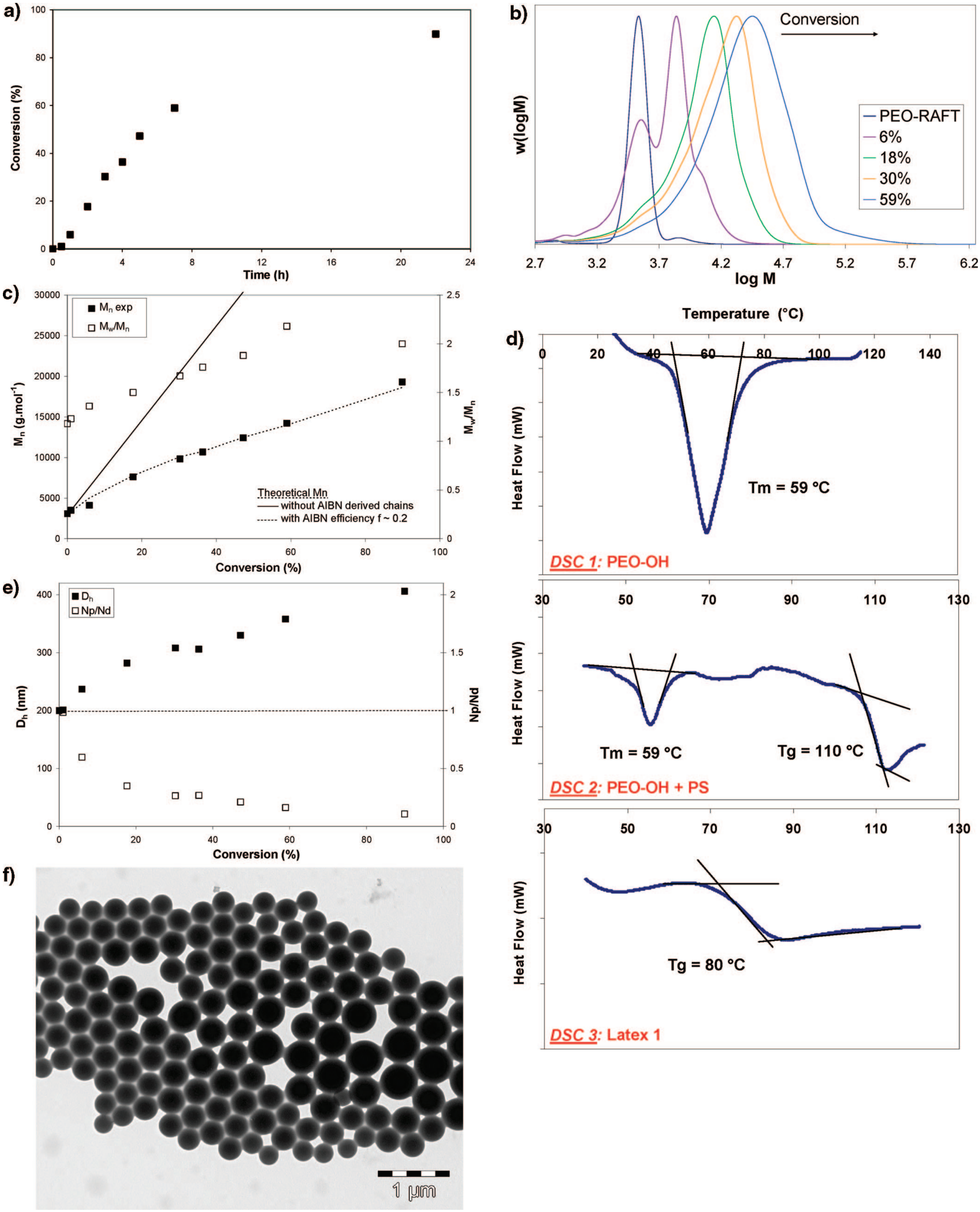

Figure 1. Miniemulsion polymerization of styrene mediated by poly(ethylene oxide)-based macromolecular agent for reversible addition-fragmentation chain transfer (PEO-RAFT), initiated by 2,2′-azobis(isobutyronitrile) (AIBN) at 75 °C (Latex 1, see Table 1). (a) Evolution of monomer conversion vs time, (b) evolution of size exclusion chromatograms with conversion, (c) number average molar mass (M_n) and polydispersity index (M_w/M_n) vs conversion (please note that the full line corresponds to theoretical M_n vs conversion without taking into account initiator derived chains, whereas the dotted line takes into account AIBN derived chains with an arbitrary AIBN efficiency = 0.2), (d) differential scanning calorimetry (DSC) measurements after the two temperature treatments carried out on [DSC1: a commercial PEO-OH. DSC2: a mixture of commercial PEO-OH (1 mg) and polystyrene (100 mg) prepared with the same theoretical weight ratio as Latex 1. DSC 3: Latex 1], (e) hydrodynamic diameter (D_h) and ratio of number of particles (N_p) to the number of initial droplets (N_d) vs conversion, and (f) transmission electron microscopy photo of the final latex.

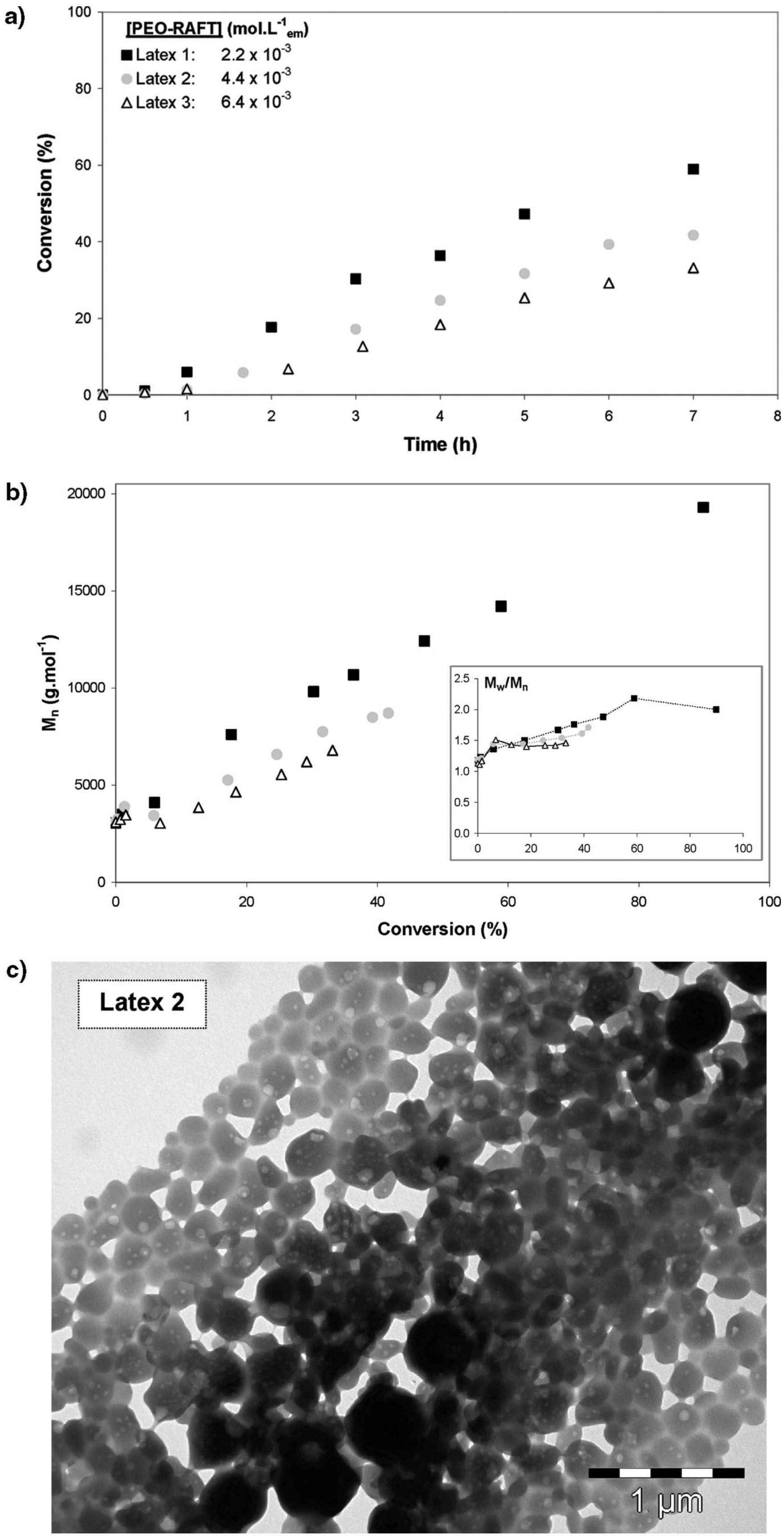

Figure 2. Influence of initial concentration of poly(ethylene oxide)-based macromolecular agent for reversible addition-fragmentation chain transfer (PEO-RAFT) (2.2×10^{-3} mol$\cdot$L$^{-1}_{\text{em}}$ (Latex 1); 4.4×10^{-3} mol$\cdot$L$^{-1}_{\text{em}}$ (Latex 2); 6.4×10^{-3} mol$\cdot$L$^{-1}_{\text{em}}$ (Latex 3)) for the PEO-RAFT mediated miniemulsion polymerization of styrene initiated by 2,2′-azobis(isobutyronitrile) (AIBN) at 75 °C. (a) Evolution of monomer conversion vs time, (b) number average molar mass (M_n) and polydispersity index (M_w/M_n) vs conversion for Latexes 1, 2, and 3, and (c) transmission electron microscopy photo of the final Latex 2 (see Table 1 for detailed experimental conditions).

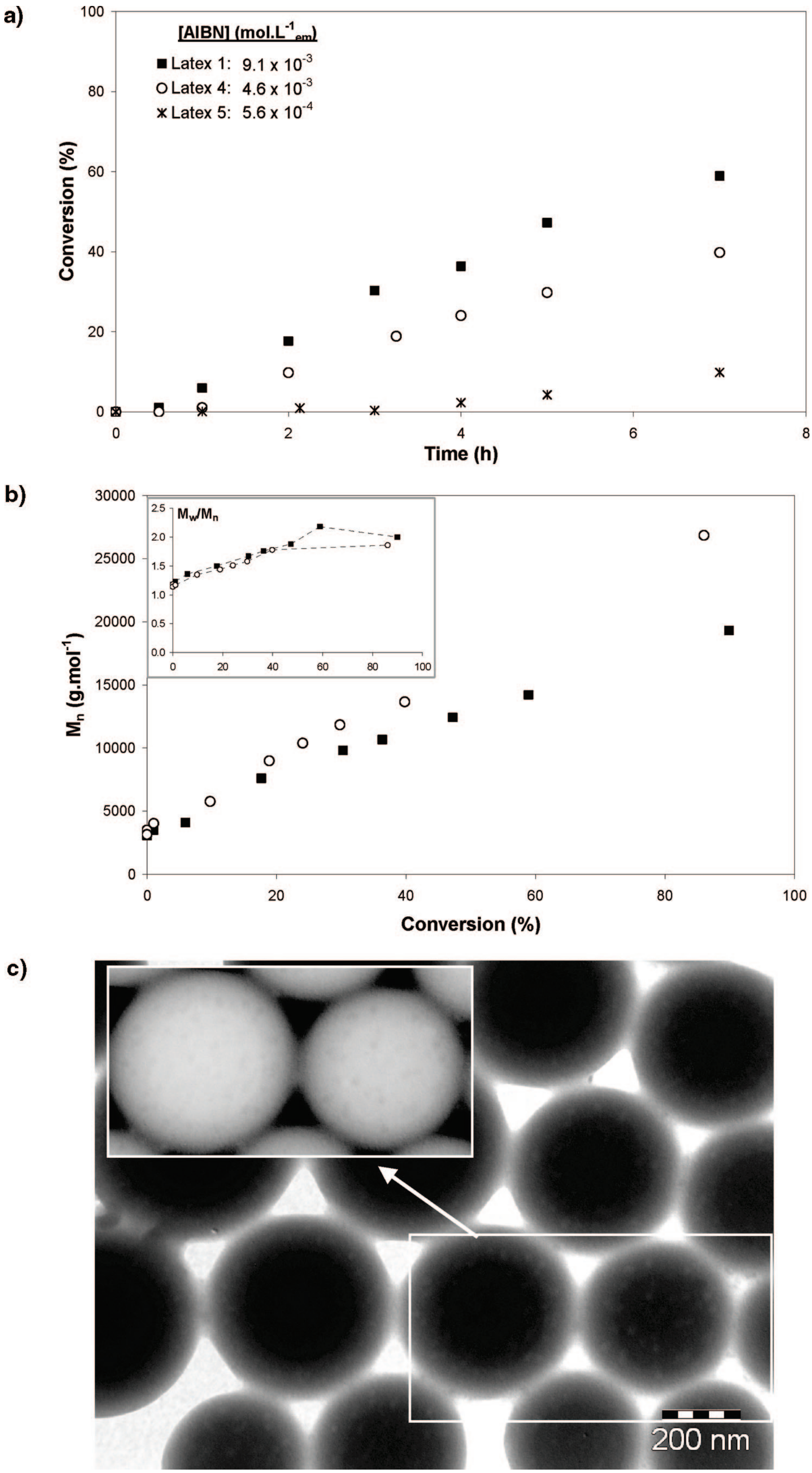

Figure 3. Influence of initial 2,2′-azobis(isobutyronitrile) (AIBN) concentration (9.1×10^{-3} mol·L^{-1}$_{em}$ (Latex 1); 4.6×10^{-3} mol·L^{-1}$_{em}$ (Latex 4); 5.6×10^{-4} mol·L^{-1}$_{em}$ (Latex 5)) for the miniemulsion polymerization of styrene mediated by poly(ethylene oxide)-based macromolecular agent for reversible addition-fragmentation chain transfer (PEO-RAFT) at 75 °C (see Table 1 for detailed experimental conditions). (a) Evolution of monomer conversion vs time, (b) number average molar mass (M_n) and polydispersity index (M_w/M_n) vs conversion for Latexes 1, 4, and 5, and (c) transmission electron microscopy photo of the final Latex 4. Please note that the contrast has been adjusted in order to enhance in the figure the lower contrast domains, which were clearly observed during the actual TEM analysis.

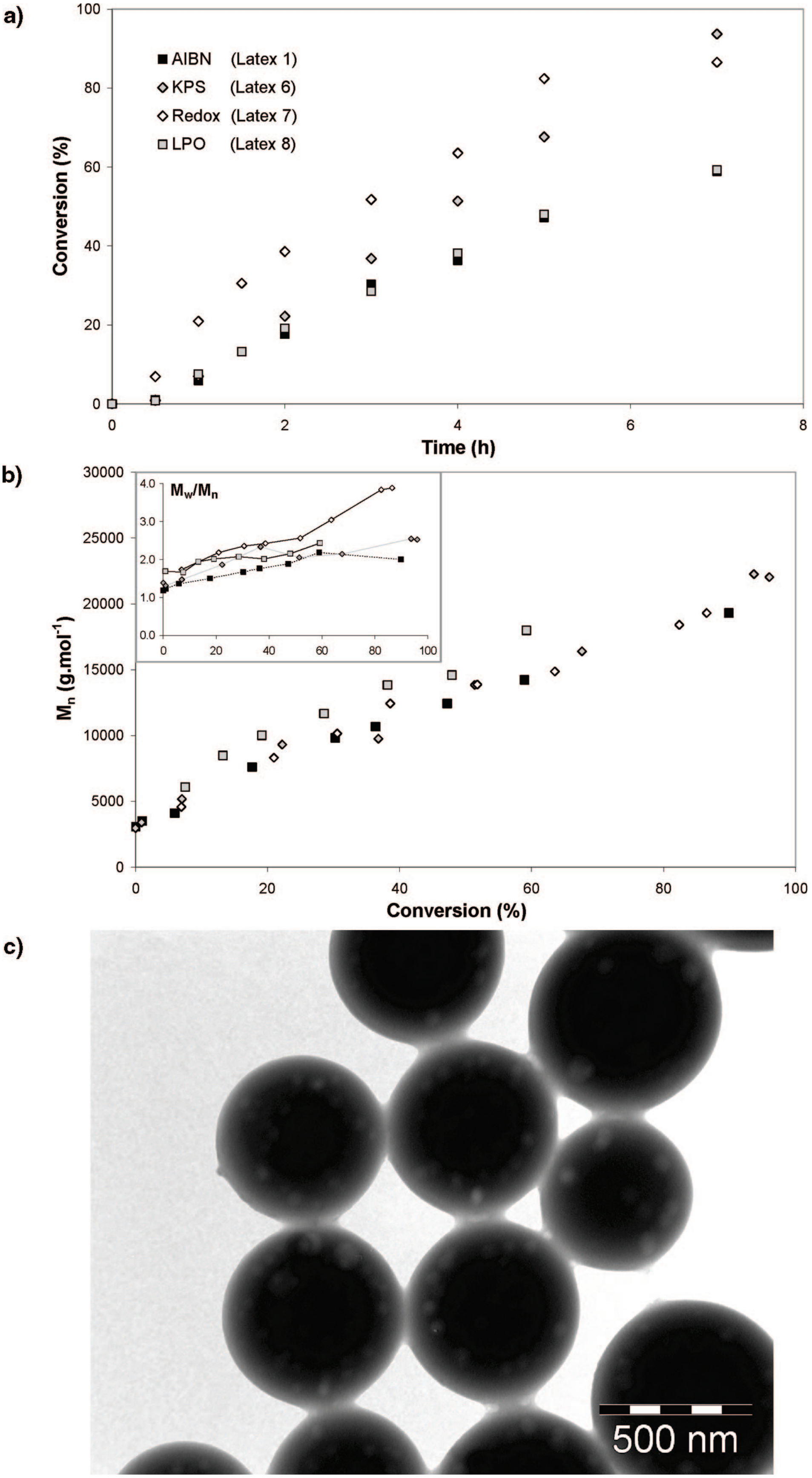

Figure 4. Influence of the type of initiator for the miniemulsion polymerization of styrene mediated by poly(ethylene oxide)-based macromolecular agent for reversible addition-fragmentation chain transfer (PEO-RAFT) at 75 °C (AIBN, Latex 1; potassium persulfate (KPS), Latex 6; KPS/ sodium metabisulfite (SMB), Latex 7; dilauroyl peroxide (LPO), Latex 8—see Table 1 for detailed experimental conditions). (a) Evolution of monomer conversion vs time, (b) number average molar mass (M_n) and polydispersity index (M_w/M_n) vs conversion, and (c) transmission electron microscopy photo of the final Latex 6.

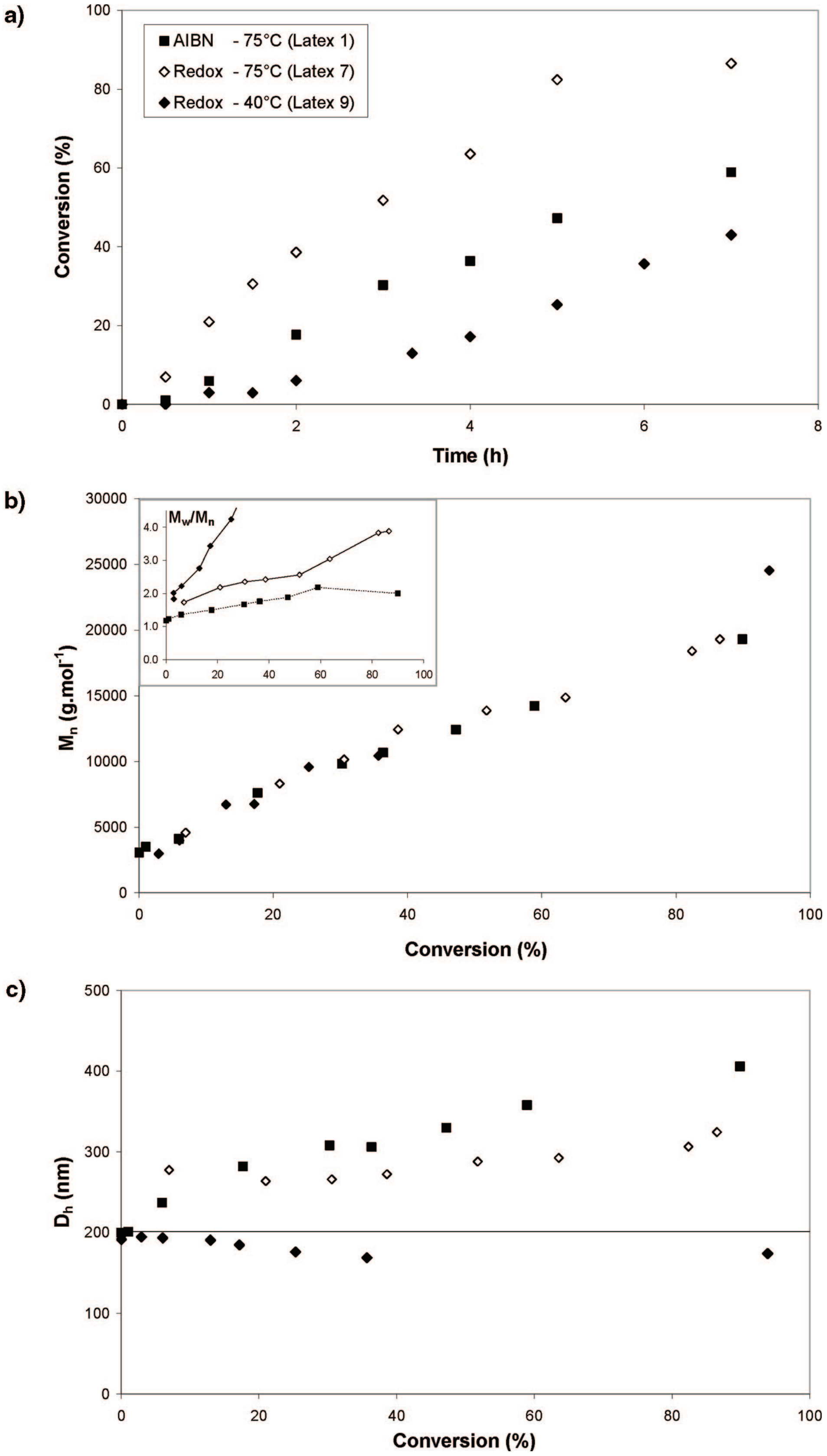

Figure 5. Influence of the polymerization temperature for the miniemulsion polymerization of styrene mediated by poly(ethylene oxide)-based macromolecular agent for reversible addition-fragmentation chain transfer (PEO-RAFT) and initiated by the redox couple potassium persulfate/ sodium metabisulfite (75 °C, Latex 7; 40 °C, Latex 9—see Table 1 for detailed experimental conditions). (a) Evolution of monomer conversion vs time and (b) number average molar mass (M_n) and polydispersity index (M_w/M_n) vs conversion. Latex 1 (AIBN) is given as a reference.

to favor an efficient nucleation. From Latexes 1 to 4, the contribution of AIBN derived chains being lowered, the molar masses increase and the polydispersity indexes decrease (Figure 3b). TEM observations of the particles formed using the two highest AIBN concentrations (Latexes 1 and 4) revealed spherical shapes with very small holes for Latex 4 (Figure 3c).

Nucleation in the system using AIBN as an initiator is associated with quite complex mechanisms as evidenced above and shown by the presence of oligomers at low conversions (distribution of the species in various loci—see Figure 1b). In an attempt to narrow the molar mass distribution, two different strategies have been investigated. First, water soluble initiators such as KPS or the redox couple KPS/sodium metabisulfite (SMB) were used to initiate the polymerization in the aqueous phase (Latexes 6 and 7 in Table 1, respectively) and rapidly locate the polymerization inside the particles. On the other hand, to lower the extent of events occurring into the aqueous phase, we also used highly water insoluble dilauroyl peroxide (LPO) (Latex 8, Table 1, water solubility[35] $= 2 \times 10^{-9}$ mol·L^{-1}). The polymerization proceeds at a significantly higher rate when using water soluble initiators (Figure 4a), the redox couple being as expected the more efficient as this system is supposed to generate radicals more rapidly than KPS alone, and it should therefore provide a more efficient nucleation of the droplets. LPO did not induce a noticeable difference in the rate of polymerization compared with AIBN. In all the cases, compared to the AIBN initiated system, molar masses increased with conversion without significant difference while the molar mass distribution was slightly broader especially with the redox system (Figure 4b). It should be noted that for the same concentration of initiator, the particles obtained with KPS (Latex 6) exhibits clear holes (Figure 4c), whereas Latex 1 (AIBN) does not. In the particular case of KPS (and for this PEO-RAFT concentration), the presence of these holes may additionally be related to the sulfate groups.[41]

Influence of the Polymerization Temperature. The last experiment consisted in decreasing the polymerization temperature in order to better fit the starting miniemulsion formation conditions. As mentioned at the beginning of this paper, although an increase in temperature to 75 °C probably led to a reorganization of the PEO-RAFT molecules between organic and aqueous phases, the obtained miniemulsion was stable for several hours at room temperature. In that respect, we decided to perform the polymerization at a temperature that would better reflect the starting arrangement of the different phases and thus probably improve the particle size distribution. The redox couple KPS/SMB was then employed to initiate the PEO-RAFT mediated miniemulsion of styrene at 40 °C. A stable latex was obtained at the end of the polymerization (23 h, 94% conversion, Latex 9, Table 1 and Figure 5a). The evolution of molar masses with conversion was very similar to the one observed at 75 °C (Figure 5b), with however a strong increase in polydispersity indices (>4) showing a rapid loss of control of the polymerization. Nevertheless, as shown by the evolution of the particle size with conversion (Figure 5c), the miniemulsion features seem to be kept with D_h values close to 180 nm (and N_p/N_d close to 1) all over the course of the polymerization. This experiment shows that a true miniemulsion polymerization of styrene mediated by PEO-RAFT can be performed with lower polymerization temperatures that do not disturb the initial partitioning of PEO-RAFT between the different phases. Particle size issue being fixed, molar mass distribution may then be improved by the use of hydrophobic initiator with low decomposition temperature. These experiments are currently under way in our laboratories.

Conclusions

The present study reported on the use of a presynthesized PEO-RAFT polymer used as both a stabilizer and a control agent to mediate the miniemulsion polymerization of styrene. After checking the ability of PEO-RAFT to stabilize a miniemulsion of styrene in water, polymerizations were undertaken at 75 °C using AIBN as initiator. DSC measurements and molar mass determinations showed that the system was living although polydispersity indices reached values up to 2.2. This rather broad molar mass distribution was indeed assigned to the presence of different populations of controlled chain length arising from the partitioning of PEO-RAFT between the aqueous phase, the droplets and the water/droplets interface. This also led to a loss of the miniemulsion features with N_p/N_d well below the expected value of 1. Complex mechanisms induced by PEO-RAFT partitioning were indeed corroborated by the presence of holes observed by TEM when PEO-RAFT concentration was raised, and likely arising from the formation of buried PEO-*b*-PS block copolymers. Attempts to improve the molar mass distribution by varying the concentration and the nature of the initiator did not work. A decrease in polymerization temperature consistent with the starting miniemulsion stability in conjunction with the use of an adequate hydrophobic initiator seemed to be the way to obtain a true miniemulsion polymerization system with a relatively constant particle diameter during the polymerization, while maintaining a good level of control.

Supporting Information Available: Figure showing the aging of the droplet diameter with time for a styrene miniemulsion. This material is available free of charge via the Internet at http://pubs.acs.org.

References and Notes

(1) Guyot, A.; Tauer, K.; Asua, J. M.; Van Es, S.; Gauthier, C.; Hellgren, A. C.; Sherrington, D. C.; Montoya-Goni, A.; Sjoberg, M.; Sindt, O.; Vidal, F.; Unzue, M.; Schoonbrood, H.; Shipper, E.; Lacroix-Desmazes, P. *Acta Polym.* **1999**, *50*, 57–66.

(2) Guyot, A.; Tauer, K. Polymerizable and Polymeric Surfactants. In *Reactions and Synthesis in Surfactants Systems*; Texter, J., Ed.; Marcel Dekker: New York, 2001; Vol. *100*, XXVIII, pp547−576.

(3) Guyot, A. *Macromol. Symp.* **2002**, *179*, 105–132.

(4) Riess, G.; Labbe, C. *Macromol. Rapid Commun.* **2004**, *25*, 401–435.

(5) Guyot, A. Apport des tensioactifs réactifs. In *Les latex synthétiques. Elaboration, Propriétés, Applications*; Pichot, C., Daniel, J. C., Eds.; Lavoisier: Paris, 2006; pp 759−783.

(6) Nagamune, T.; Ueda, A.; Nagai, S. *J. Appl. Polym. Sci.* **1996**, *62*, 359–365.

(7) Vidal, F.; Guillot, J.; Guyot, A. *Polym. Adv. Technol.* **1995**, *6*, 473–479.

(8) Wilkinson, T. S.; Boonstra, A.; Montoya-Goni, A.; van Es, S.; Monteiro, M. J.; German, A. L. *J. Colloid Interface Sci.* **2001**, *237*, 21–27.

(9) Fifield, C. C.; Fitch, R. M. *C. R. Chim.* **2003**, *6*, 1305–1312.

(10) Bourgeat-Lami, E.; Guyot, A. *Polym. Bull.* **1995**, *35*, 691–696.

(11) Bourgeat-Lami, E.; Guyot, A. *Colloid Polym. Sci.* **1997**, *275*, 716–729.

(12) Miyazaki, H.; Terada, K.; Sato, T.; Maruyama, H.; Okaya, T. *J. Appl. Polym. Sci.* **1996**, *60*, 2149–2157.

(13) Vidal, F.; Gilbert, R. G. *Macromol. Chem. Phys.* **1996**, *197*, 1835–1840.

(14) Monteiro, M. J.; Bussels, R.; Wilkinson, T. S. *J. Polym. Sci., Part A: Polym. Chem.* **2001**, *39*, 2813–2820.

(15) Matyjaszewski, K.; Davis, T. P., Eds. *Handbook of Radical Polymerization.* ; Wiley Interscience, John Wiley and Sons Inc.: New York, 2002.

(16) Matyjaszewski, K., Ed. *Advances in Controlled/Living Radical Polymerization* American Chemical Society: Washington DC, 2003; Vol. *854*.

(17) Zetterlund, P. B.; Kagawa, Y.; Okubo, M. *Chem. Rev.* **2008**, *108*, 3747–3794.

(18) Cunningham, M. F. *Prog. Polym. Sci.* **2008**, *33*, 365–398.

(19) Barner-Kowollik, C., Ed. *Handbook of RAFT Polymerization.* Wiley-VCH: Weinheim, Germany, 2008.

(20) Fréal-Saison, S.; Save, M.; Bui, C.; Charleux, B.; Magnet, S. *Macromolecules* **2006**, *39*, 8632–8638.

(21) Ganeva, D. E.; Sprong, E.; de Bruyn, H.; Warr, G. G.; Such, C. H.; Hawkett, B. S. *Macromolecules* **2007**, *40*, 6181–6189.

(22) Pham, B. T. T.; Nguyen, D.; Ferguson, C. J.; Hawkett, B. S.; Serelis, A. K.; Such, C. H. *Macromolecules* **2003**, *36*, 8907–8909.

(23) Luo, Y.; Gu, H. *Macromol. Rapid Commun.* **2006**, *27*, 21–25.

(24) Lu, F.; Luo, Y.; Li, B. *Macromol. Rapid Commun.* **2007**, *28*, 868–874.

(25) Ferguson, C. J.; Hughes, R. J.; Pham, B. T. T.; Hawkett, B. S.; Gilbert, R. G.; Serelis, A. K.; Such, C. H. *Macromolecules* **2002**, *35*, 9243–9245.

(26) Ferguson, C. J.; Hughes, R. J.; Nguyen, D.; Pham, B. T. T.; Gilbert, R. G.; Serelis, A. K.; Such, C. H.; Hawkett, B. S. *Macromolecules* **2005**, *38*, 2191–2204.

(27) Boŏvić-Vukić, J.; Manon, H. T.; Meuldijk, J.; Koning, C.; Klumperman, B. *Macromolecules* **2007**, *40*, 7132–7139.

(28) Tichagwa, L.; Götz, C.; Tonge, M.; Sanderson, R.; Pasch, H. *Macromol. Symp.* **2003**, *193*, 251–260.

(29) Manguian, M.; Save, M.; Charleux, B. *Macromol. Rapid Commun.* **2006**, *27*, 399–404.

(30) dos Santos, A. M.; Pohn, J.; Lansalot, M.; D'Agosto, F. *Macromol. Rapid Commun.* **2007**, *28*, 1325–1332.

(31) Bernard, J.; Save, M.; Arathoon, B.; Charleux, B. *J. Polym. Sci., Part A: Polym. Chem.* **2008**, *46*, 2845–2857.

(32) Ji, J.; Yan, L.; Xie, D. *J. Polym. Sci., Part A: Polym. Chem.* **2008**, *46*, 3098–3107.

(33) Rieger, J.; Stoffelbach, F.; Bui, C.; Alaimo, D.; Jérôme, C.; Charleux, B. *Macromolecules* **2008**, *41*, 4065–4068.

(34) Bathfield, M.; D'Agosto, F.; Spitz, R.; Charreyre, M.-T.; Pichot, C.; Delair, T. *Macromol. Rapid Commun.* **2007**, *28*, 1540–1545.

(35) Alduncin, J. A.; Forcada, J.; Asua, J. M. *Macromolecules* **1994**, *27*, 2256–2261.

(36) Barner-Kowollik, C.; Buback, M.; Charleux, B.; Coote, M. L.; Drache, M.; Fukuda, T.; Goto, A.; Klumperman, B.; Lowe, A. B.; McLeary, J. B.; Moad, G.; Monteiro, M. J.; Sanderson, R. D.; Tonge, M. P.; Vana, P. *J. Polym. Sci., Part A: Polym. Chem.* **2006**, *44*, 5809–5831.

(37) Luo, Y.; Wang, R.; Yang, L.; Yu, B.; Li, B.; Zhu, S. *Macromolecules* **2006**, *39*, 1328–1337.

(38) Okubo, M.; Kobayashi, H.; Matoba, T.; Oshima, Y. *Langmuir* **2006**, *22*, 8727–8731.

(39) Kobayashi, H.; Miyanaga, E.; Okubo, M. *Langmuir* **2007**, *23*, 8703–8708.

(40) Tauer, K. *Macromolecules* **2006**, *39*, 2007–2009.

(41) Tauer, K.; Deckwer, R.; Kühn, I.; Schellenberg, C. *Colloid Polym. Sci.* **1999**, *277*, 607–626.

(42) Tauer, K.; Antonietti, M.; Rosengarten, L.; Müller, H. *Macromol. Chem. Phys.* **1998**, *199*, 897–908.

(43) Brandrup, J.; Immergut, E. H.; Grulke, E. A.; Abe, A.; Bloch, D. R., Eds. *Polymer Handbook*, 4th ed.; John Wiley and Sons, Inc.: New York, 1999.

(44) Gilbert, R. G., Ed. *Emulsion Polymerization: a Mechanistic Approach.* Academic Press: London, 1995.

(45) Lansalot, M.; Davis, T. P.; Heuts, J. P. A. *Macromolecules* **2002**, *35*, 7582–7591.

MA802117H